Queensland University of Technology
Brisbane Australia

This may be the author's version of a work that was submitted/accepted for publication in the following source:

Tesfamichael, Tuquabo, Cetin, C., Piloto, Carlo, Arita, Masashi, & Bell, John
(2015)
The effect of pressure and W-doping on the properties of ZnO thin films for NO2 gas sensing.
Applied Surface Science, *357*(Part A), pp. 728-734.

This file was downloaded from: https://eprints.qut.edu.au/95150/

© Consult author(s) regarding copyright matters

This work is covered by copyright. Unless the document is being made available under a Creative Commons Licence, you must assume that re-use is limited to personal use and that permission from the copyright owner must be obtained for all other uses. If the document is available under a Creative Commons License (or other specified license) then refer to the Licence for details of permitted re-use. It is a condition of access that users recognise and abide by the legal requirements associated with these rights. If you believe that this work infringes copyright please provide details by email to qut.copyright@qut.edu.au

License: Creative Commons: Attribution-Noncommercial-No Derivative Works 4.0

Notice: *Please note that this document may not be the Version of Record (i.e. published version) of the work. Author manuscript versions (as Submitted for peer review or as Accepted for publication after peer review) can be identified by an absence of publisher branding and/or typeset appearance. If there is any doubt, please refer to the published source.*

https://doi.org/10.1016/j.apsusc.2015.08.248

Applied Surface Science 357 (2015) 728–734

The effect of pressure and W-doping on the properties of ZnO thin films for NO_2 gas sensing

T. Tesfamichael[a*], C. Cetin[b], C. Piloto[a], M. Arita[c], J. Bell[a]

[a]Science and Engineering Faculty, Queensland University of Technology
2 George Street, Brisbane, 4000, QLD Australia

[b]Istanbul Technical University, Department of Mechanical Engineering,
Istanbul, Turkey
[c]Laboratory of Nanoscience and Materials, Hokkaido University,
Kita 14, Nishi 9, Kita-Ku, Sapporo, 060-0814, Japan

*Corresponding author: Phone: +61-7-31381988
Fax: +61-7-31381516
email: t.tesfamichael@qut.edu.au

Abstract

Pure and W-doped ZnO thin films were obtained using magnetron sputtering at working pressures of 0.4 Pa and 1.33 Pa. The films were deposited on glass and alumina substrates at room temperature and subsequently annealed at 400°C for 1 hour in air. The effects of pressure and W-doping on the structure, chemical, optical and electronic properties of the ZnO films for gas sensing were examined. From AFM, the doped film deposited at higher pressure (1.33 Pa) has spiky morphology with much lower grain density and porosity compared to the doped film deposited at 0.4 Pa. The average gain size and roughness of the annealed films were estimated to be 65 nm and 2.2 nm, respectively with slightly larger grain size and roughness appeared in the doped films. From XPS the films deposited at 1.33 Pa favored the formation of adsorbed oxygen on the film surface and this has been more pronounced in the doped film which created active sites for OH adsorption. As a consequence the W-doped film deposited at 1.33 Pa was found to have lower oxidation state of W (35.1 eV) than the doped film deposited at 0.4 Pa (35.9 eV). Raman spectra indicated that doping modified the properties of the ZnO film and induced free-carrier defects. The transmittance of the samples also reveals an enhanced free-carrier density in the W-doped films. The refractive index of the pure film was also found to increase from 1.7 to 2.2 after W-doping whereas the optical band gap only slightly increased. The W-doped ZnO film deposited at 0.4 Pa appeared to have favorable properties for enhanced gas sensing. This film showed significantly higher sensing performance towards 5-10 ppm NO_2 at lower operating temperature of 150°C most dominantly due to increased free-carrier defects achieved by W-doping.

Keywords

Nanostructure; ZnO thin films; W-doping; sputtering pressure; NO_2 gas sensors

Applied Surface Science 357 (2015) 728–734

1. Introduction

Today nanostructured semiconducting metal oxide thin films have received greatest attention due to their properties that are different from those of their bulk counterparts. With the advancement of modern technologies, well controlled processing and development techniques can produce metal oxide thin films with desirable physical, chemical, electrical, optical and other properties suitable in various applications [1, 2]. Among the metal oxides, nanostructured ZnO thin film has been investigated extensively due its wide range of applications including optoelectronics, piezoelectricity, catalysis, and gas sensor devices [3-5]. Several techniques have been used to deposit pure and doped nanostructured ZnO thin films including sol-gel, CVD, ultrasonic spray pyrolysis, pulsed laser deposition, physical vapour deposition, thermal oxidation [6-13]. While all these techniques have their own advantages and limitations, better control of film quality and properties can be obtained using PVD techniques [5, 14-20]. From the various PVD techniques, magnetron sputtering has simplified fabrication steps with well controlled deposition variables to essentially grow high quality films. In the literature, the influences of sputter deposition parameters including partial pressure, sputtering power, reactive gas species, temperature, etc. on the properties of pure and doped ZnO films on various substrates have been investigated [2, 3, 21, 22]. When modification of the as-deposited films for specific application has become desirable, post-annealing heat treatments are commonly applied to achieved various film characteristics [23-26]. Several attempts have been made to enhance the gas sensing performance of ZnO through the optimization of nanostructural morphology, grain shape and size, crystalline nature, film thickness and porosity, impurities and defects [27-29]. Defects such as oxygen vacancies are inherent in most metal oxides including ZnO and this creates n-type semiconducting material. As the metal oxides approach to stoichiometry, however, oxygen vacancies are reduced and the conductivity of the oxide becomes extremely low (high resistance) and gas-sensing measurements become difficult. Doping can effectively modify the stoichiometric properties of ZnO film and increases oxygen vacancies and free-carrier density to enhance gas sensing performance [30-33]. Several methods such as laser deposition, CVD, sol-gel and sputtering were used to deposit W-doped ZnO films [34-37] but none of these films has been investigated for gas sensing.

In this paper pure and W-doped ZnO films were obtained using magnetron co-sputtering at two different pressures of 0.4 Pa and 1.33 Pa using low sputtering power. The films were developed at room temperature and subsequently annealing at 400^{o}C for 1 hour in air. The effects of sputtering pressure and W-doping on the structure, chemical, optical and electronic properties of ZnO films for gas sensing were examined. The morphology, composition and crystallinity nature of the films were analysed using atomic force microscope (AFM), X-Ray Photoelectron Spectroscopy (XPS) and Raman Spectroscopy. The thickness and refractive index of the films were obtained using Ellipsometer and the measured thicknesses were verified using Mechanical Stylus Profilometer. The optical properties of the films were characterized using UV-Vis-NIR spectrophotometer and from the measurements the optical band gap was obtained. Gas sensing

measurements of the different samples towards NO_2 of various concentrations (1-10 ppm) at different operating temperatures (150-300°C) were carried out. From the measurements the performance of the sensors inclduing response amplitude (sensitivity), response and recovery times were evaluated.

2. Experimental Methods

2.1. Sample Preparation

Magnetron sputtering (PVD 75 K.J. Lesker with 4 targets of 50 mm diameter) was used to produce pure and W-doped ZnO thin films from high purity zinc oxide (99. 9%) and tungsten (99.95%) targets. After the chamber was evacuated to a base pressure of 8.2 x 10^{-6} Pa, Ar gas (99.99% purity) was introduced into the chamber and maintained at the desired working pressure. The pure ZnO films were produced from the ZnO target using RF power of 30 W. Doping was done by co-sputtering ZnO and W targets using 30 W RF and 10 W DC power, respectively. Several films were obtained on glass and alumina (8 x 8 mm) substrates at sputtering pressure of 0.4 Pa and 1.33 Pa. The alumina (8 x 8 mm) consisted of pre-printed Pt-interdigitated electrodes with line width 100 μm and height 300 nm has been used for gas sensing measurements. The substrate holder was fixed at a distance of 150 mm from the target and was allowed to rotate at 20 rpm to keep the uniformity of the films. All the samples were deposited at room temperature (24°C) for 120 minutes and subsequently annealed at 400°C for 1 hour in air. Prior to the film deposition, 5 minutes pre-sputtering time was allowed to remove any surface contamination from the source target and also to ensure stability of the sputtering conditions. Only four samples identified by their doping and sputtering pressure as shown in Table 1 were closely examined for gas sensing.

2.2. Film Characterization

Film thickness measurements were performed using M-2000 Ellipsometer (J. A. Woollam Co., Inc.) and the results were confirmed with mechanical stylus profilometer (Bruker Dektak XT). Ellipsometric measurements of the samples on glass substrates were also carried out to determine the refractive indices of the films. The surface morphologies of the films on alumina substrates before and after annealing were obtained using AFM (Nanocute SII) in tapping mode configuration with nominal tip diameter of 10 nm. All the samples were scanned over 1 μm x 1 μm area.

Raman spectroscopy has been employed to analyse the effect of W-doping on the structural and chemical nature of the ZnO film. WITec Raman confocal microscope with laser excitation source of 633 nm wavelength was used. The laser was focused on the surface of the films to reduced background effect from the substrate. Raman shift of the films between the wavenumbers 200 to 700 cm^{-1} has been examined. The chemical makeup and composition of the pure and W-doped ZnO film were obtained from XPS spectra. The XPS data was acquired from

Shimadzu ESCA-3400 using non-monochromatic MgKα X-rays (10 kV, 20 mA) over the binding energy range of 0 to 1100 eV. Survey (wide) and high resolution scans were performed at steps of 1 eV and 0.1 eV, respectively. All the binding energies were corrected using C 1s peak of graphite (284.8 eV) as a reference. The peak analyses were carried out by using XPSpeak41. The optical properties of the films on glass substrates were measured using Cary 50 UV-Vis-NIR spectrophotometer in the wavelength range 300 to 1100 nm at normal angle of incidence.

Table 1: Sputtering parameters (power, pressure and time) used for the deposition of the pure and W-doped ZnO films.

Specimen	ZnO RF power (W)	W DC power (W)	Time (min)	Pressure (Pa)
ZnO (0.4Pa)	30	0	120	0.4
ZnO (1.33Pa)	30	0	120	1.33
ZnO:W (0.4Pa)	30	10	120	0.4
ZnO:W (1.33Pa)	30	10	120	1.33

2.3. Gas Sensing Measurement

Gas sensing measurements of the four samples shown in Table 1 towards NO_2 were carried out in a flow through chamber using a high precision multi-channel gas testing system. The system includes an 1100 cc volume test chamber capable of testing four sensors in parallel, an eight high precision mass flow controllers (MKS 1479A) to regulate the gas mixture, an eight channel MFC processing unit (MKS 647C), a pico-ammeter (Keithley 6487) and a climatic chamber to control the temperature. The measurements were performed in a chamber with different target gas concentrations of 1, 5 and 10 ppm at the operating temperatures of 150-300°C. The exact concentration of the target gas was obtained by mixing with synthetic air while maintaining a total constant flow rate of 200 sccm (mL/min). The concentration range has been selected within the threshold limit values acceptable in various applications [38]. The response of the films was evaluated by measuring the sensors resistance variation using bias voltage of 1 V. The desired operating temperature was regulated by applying voltage to a micro-ceramic heating element having resistance of 44 ohms (Sakaguchi MS-3). The duration for each gas exposure was 5 min with reasonable 20 min time allowed for the recovery of the sensors prior to the next exposure. The sensor response amplitude (i.e. sensitivity, S) was used as the measure of sensor response and is defined as a positive quantity and for oxidizing target gas (e.g. NO_2):

$$S= (R-R_{air})/R_{air}=\Delta R/R_{air} \quad (1)$$

where R_{air} is the steady state resistance value in the reference air and R the final resistance of the sensor when exposed to the target gas achieved within a reasonable time (5 min) [39]. The

response time was determined by considering the time required for the sensor to reach 90% of the final S value after exposed to the target gas. Similarly the recovery time of the sensor was also obtained from the time the sensor requires to recover the 90% of the maximum S value so it reached 10% above the baseline resistance after switching off the target gas.

3. Results and discussion

As shown in Table 2, the film thickness of the pure and W-doped ZnO films as measured using Ellipsometer were about 100 nm thick and the values were verified using the mechanical stylus profiler. From the data, the deposition rates of the films were calculated and found to be less than 1 nm/min. Results show that the deposition rate of the doped films appeared slightly higher than the corresponding pure films. However, there is no clear correlation between the deposition rate and sputtering pressure.

Fig. 1 shows AFM surface morphologies (1 μm x 1 μm) of the as-deposited pure and W-doped ZnO films at sputtering pressures of 0.4 Pa and 1.33 Pa. From the images both doping and sputtering pressure have significant effect on the morphology of the ZnO films [2]. As shown in Fig. 1, the as-deposited pure ZnO films have predominately amorphous characteristics when deposited at lower sputtering pressure (0.4 Pa), whereas doping and/or increasing pressure (1.33 Pa) improved the formation of ZnO granules. Looking at the doped films, the film deposited at 1.33 Pa (Fig. 1d) appeared to produce spiky morphology with much lower grain density and porosity compared to the doped film deposited at 0.4 Pa (Fig. 1c).

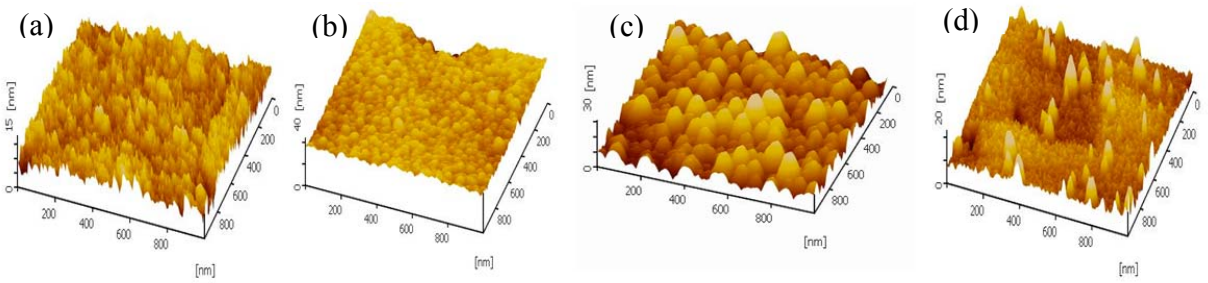

Fig. 1 AFM morphology of as-deposited films on alumina electrodes: (a) ZnO (0.4 Pa), (b) ZnO (1.33 Pa), (c) ZnO:W (0.4 Pa), and (d) ZnO:W (1.33 Pa).

Annealing of the as-deposited samples at 400°C for 1 hour promoted the formation of nanostructured grains. Defects were also observed in all the annealed films which can be useful for enhancing gas sensing performance. From the AFM images (Fig. 2a-d), the gain sizes of the pure and doped films appeared similar with slightly higher size found in the doped films as shown in Table 2. Analysis of the images indicated that the average grain size and surface roughness of the films were 65 nm and 2.2 nm, respectively. When the morphologies of the annealed films in Fig. 2 are compared, the W-doped ZnO film sputtered at 1.33 Pa (Fig. 2d) has fewer grains and the protruding on the film surface.

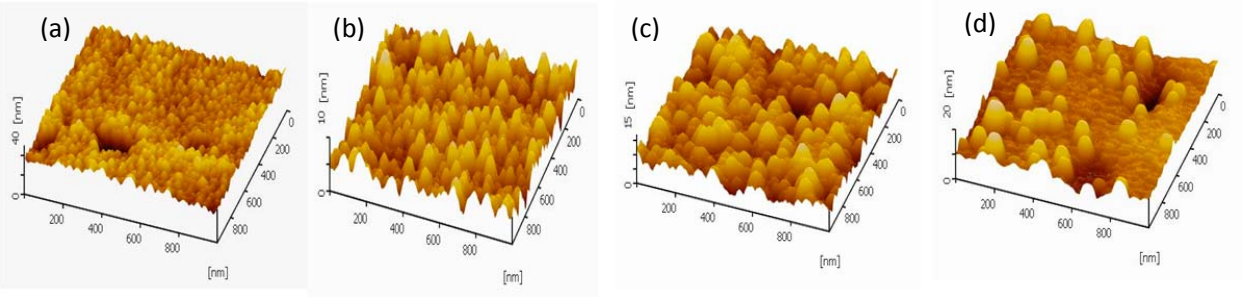

Fig. 2 AFM morphology of annealed films on alumina electrodes: (a) ZnO (0.4 Pa), (b) ZnO (1.33 Pa), (c) ZnO:W (0.4 Pa), and (d) ZnO:W (1.33 Pa).

Table 2: Film thickness (t), deposition rate (f), grain size (D) and surface roughness (R_a) of pure and W-doped ZnO films. Ellipsometer was used to measure t whereas D and R_a are obtained using AFM.

Sample	t (nm)	f (nm/min)	D (nm)	R_a (nm)
ZnO (0.4 Pa)	94	0.78	64	2.6
ZnO (1.33 Pa)	99	0.83	62	2.1
ZnO:W (0.4 Pa)	110	0.92	67	1.9
ZnO:W (1.33 Pa)	102	0.85	70	2.1

Raman spectroscopy has been employed to analyse the chemical and crystalline nature of the films as there was no diffraction observer from XRD grazing incidence measurement. Raman spectra of the annealed films were very weak and thus the highest Raman intensity was observed using confocal microscope. As shown in Fig. 3, the pure film deposited at 1.33 Pa has shown sharp Raman characteristics at wavenumber of 440 cm^{-1}. This typical peak is usually assigned in the literature to the Raman active transverse (TO) phonon mode [4]. The position of the optical phonon mode indicated nanocrystalline ZnO films having wurtzite hexagonal phase. All the films have shown a broader Raman peak centred at about 580 cm^{-1}. The boarding occurred due to the influence of Raman peak of glass substrate at around 554 cm^{-1}. This additional mode at 580 cm^{-1} is related to defect-induced modes such as oxygen vacancies, Zn interstitials and free-carrier defects induced by dopants. The enhanced intensity of this mode (580 cm^{-1}) in the doped films indicated that W-dopant has induced higher amount of free-carrier defects, most probably due to breakdown of the translational crystalline symmetry of the pure films [40, 41]. The Raman peak at around 800 cm^{-1} found in only the W-doped films is related to tungsten oxide [35].

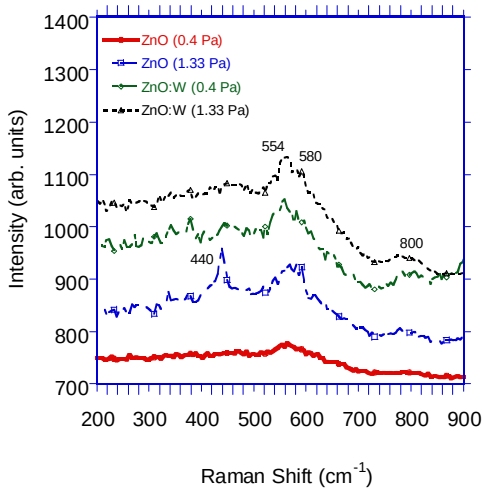

Fig. 3 Raman spectra of annealed pure and W-doped ZnO films on glass substrates sputtered at 0.4 Pa and 1.33 Pa.

From XPS survey scans, peaks of Zn, O, and C were observed in all of the films. In addition W was found in the co-sputtered films. The C signal is most likely from the surface contamination and no thus further analysis was done on it. The high resolution XPS spectra of Zn 2p, O 1s and W 4f were fitted to the experimental data as shown in Fig. 4. In the figure, the open circles are experimental data, the solid lines represent the fitted and deconvoluted curves by using Gaussian-Lorentzian function, whereas the broken lines are Shirley-type background. Two core levels of Zn 2p peak positions that belong to Zn $2p_{3/2}$ and Zn $2p_{1/2}$ were found in all the samples as shown in Fig. 4a. The binding energy difference between the two Zn 2p core levels in all the films is exactly 23.1 eV. However, the intensity of the films deposited at 1.33 Pa appeared lower than the films deposited at 0.4 Pa and the reduction is more apparent in the doped film. The Zn $2p_{3/2}$ peak position of the pure and doped films deposited at 0.4 Pa remained the same at 1022.6 eV but larger than the stoichiometric ZnO (1021.7 eV) [42]. From the films deposited at 1.33 Pa, a significant shift in the peak positon of the pure film (1022.9 eV) was observed after W-doped (1022.0 eV) due to a change in the oxidation state of the film. From the above results, Zn existed only in the oxidised state as no peak of metallic Zn (1021.5 eV) was detected. Identification of such oxidation states using the binding energy of Zn 2p is not always obvious and has been verified using the corresponding components of O 1s peaks [43] as discussed below.

In Fig. 4b, the deconvoluted spectra of O 1s show the presence of two different peaks in all the samples. The sharp peak centred at around 530.8 eV is associated with O-Zn bonding of wurtzite structure and appeared dominant in the films sputtered at 0.4 Pa. The intensity and sharpness of this peak were reduced in the films sputtered at 1.33 Pa. The peak centred at 532.7±0.5 eV is dominant in the W-doped film deposited at 1.33 Pa and this can be attributed to adsorbed oxygen [44, 45]. This doped film has also shown weak O 1s shoulder at 527.7 eV and according to

literature it was assigned to OH species [46]. Further investigation of the films shows two typical electronic core levels of W 4f that belong to W $4f_{5/2}$ and W $4f_{7/2}$ in the doped films (see Fig. 4c). The W $4f_{7/2}$ peak positions of the W-doped films sputtered at 1.33 Pa and 0.4 Pa are located at 35.1 eV and 35.9 eV, respectively. The difference between the W $4f_{7/2}$ and corresponding W $4f_{5/2}$ peaks in both doped samples is 2.5 eV which indicated the bonding of W with oxygen in the ZnO lattice [47]. The binding energy of the film deposited at 0.4 Pa (35.9 eV) is positioned near the binding energy of stoichiometric WO_3 (35.6 eV) with W in its W^{6+} oxidized state but lower oxidation state of W (35.1 eV) was observed in the film deposited at 1.33 Pa. From the above analyses it can be concluded that the films deposited at 1.33 Pa favoured the formation of adsorbed oxygen on the film surface and this has been more pronounced in the doped film which created active site for OH adsorption.

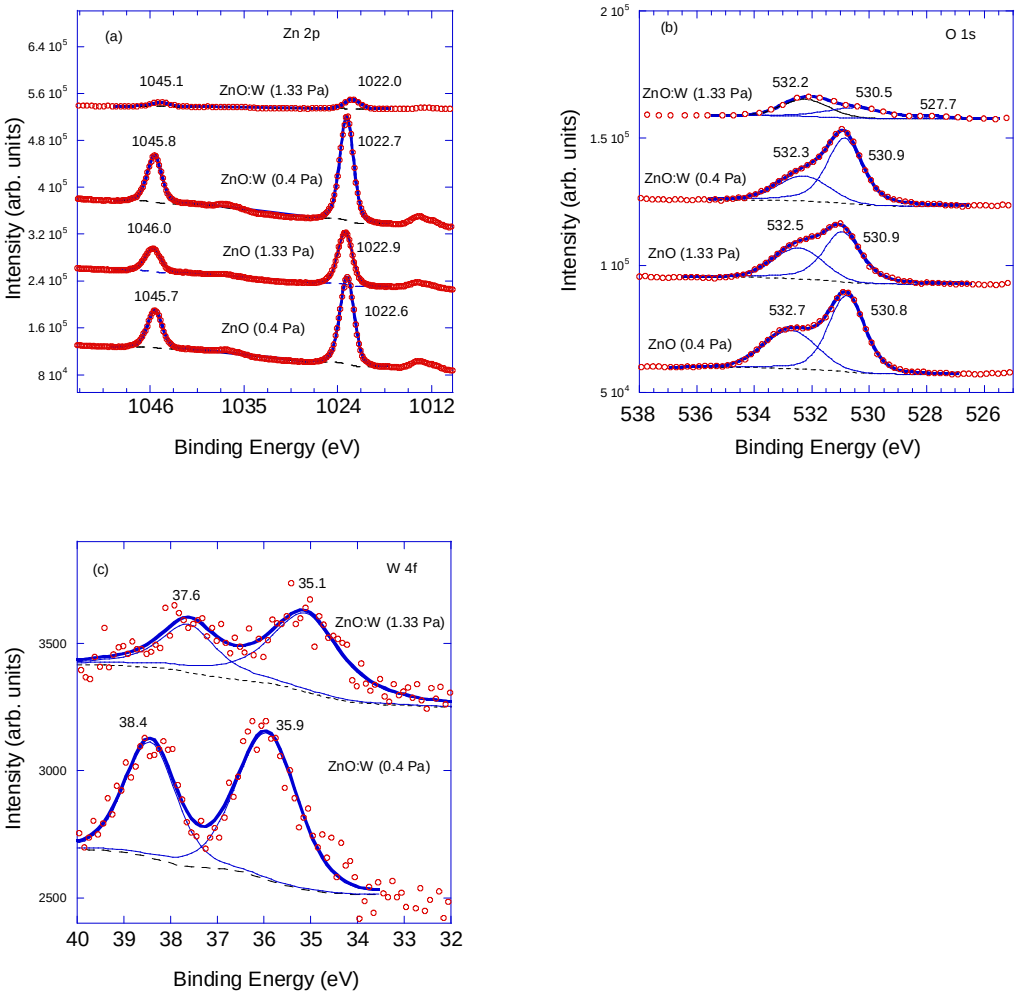

Fig. 4 XPS high resolution spectra of pure and W-doped ZnO thin films. (a) Zn 2p, (b) O 1s and (c) W 4f. The heavy lines are fitted curves.

Using Ellipsometry the refractive indices of the films in the visible wavelength (632.8 nm) were obtained. The values of the pure films (1.7-1.9) were increased after W-doping (2.0-2.2) as shown in Table 3. This may be due to an increase in free-carrier density of the pure films after doping with W. The refractive indices of the W-doped films were found similar to Al-doped ZnO films reported elsewhere [48]. The optical properties of the films on glass substrate in the UV-Vis-NIR wavelength range (300-1100 nm) are shown in Fig. 5. From Fig. 5a, the transmittance of the pure films deposited at 0.4 Pa and 1.33 Pa appeared similar, with higher transmittance in the visible and NIR but a sharp drop below 400 nm. After doping, the transmittance of the films in the visible and NIR were reduced but slightly increased in the UV (<400 nm), causing minor shifted on the onset of transmittance to shorter wavelength and this can be due to the increased number of free-carrier density. The visible transmittance (T_{vis},) values were calculated by weighting the spectrum of each film to the corresponding visible intensity for air mass 1.5. The pure ZnO films were found to be fairly transparent having visible transmittance in excess of 70% but less than the glass substrate (81%) as shown in Table 3. The weighted solar transmittance of doped films was reduced to less than 67%. The reflectance of all the films remained fairly constant with weighted visible reflectance (R_{vis}) of about 15%.

Table 3: Refractive index (n), visible transmittance (T_{vis}), film thickness (t) and optical band gap (E_g) of pure and W-doped ZnO films. The film resistance at 250°C is also shown.

Specimen	n	T_{vis} (%)	t (nm)	E_g (eV)	Film Resistance at 250°C *(kΩ)*
ZnO (0.4 Pa)	1.7	71	94	3.40	6.3
ZnO (1.33 Pa)	1.9	72	99	3.53	10.3
ZnO:W (0.4 Pa)	2.2	64	110	3.78	1698
ZnO:W (1.33 Pa)	2.0	67	102	3.80	463348

The optical band gaps (E_g) of the films were evaluated from the transmittance spectra (Fig. 5a) and Table 3 using the relationship between the absorption coefficients (α) and the photon energy (hν) for direct band gap materials such as ZnO:

$$(\alpha h\nu)^2 = A(h\nu - E_g), \quad (2)$$

where, A is a constant and is a function of refractive index and effective mass of electron and hole. Linear extrapolation of the $(\alpha h\nu)^2$ *vs* $h\nu$ plot to the energy axis (α=0) gives the optical band gap [49]. The optical absorption coefficient (α) at incident photon energy ($h\nu$) was obtained using the relationship:

$$\alpha\, t = \ln((1-R_{vis})/T_{vis}), \quad (3)$$

where t, T_{vis}, R_{vis} are the thickness, visible transmittance and reflectance of the films, respectively. As shown in Table 3, the optical band gap slightly increased when W was

incorporate into the ZnO film [50] and this is well described by the Burstein–Moss effect. The optical band gaps of the W-doped ZnO films obtained in this work are found to be within the range of Al-doped ZnO films developed by RF-sputtering [51] but slightly larger than the band gap energy of W-doped ZnO films prepared by CVD [35]. Although the method of film preparation can have an effect on the optical band gap, other factors such as film thickness also have significant influence. To determine the influence of film thickness on the optical band gap, a number of un-doped ZnO films of different thicknesses were deposited at 0.4 Pa. Fig. 5b shows the shift of the onset of transmittance to the longer wavelength with increasing film thickness. As shown in the inset of the figure, the optical band gap of the pure ZnO film decreases with increasing film thickness but this is less pronounce when the film thickness is above 90 nm. The samples analysed in Table 3 have film thicknesses between 94-110 nm and hence the effect of film thickness variation on the optical band gap can be minimum.

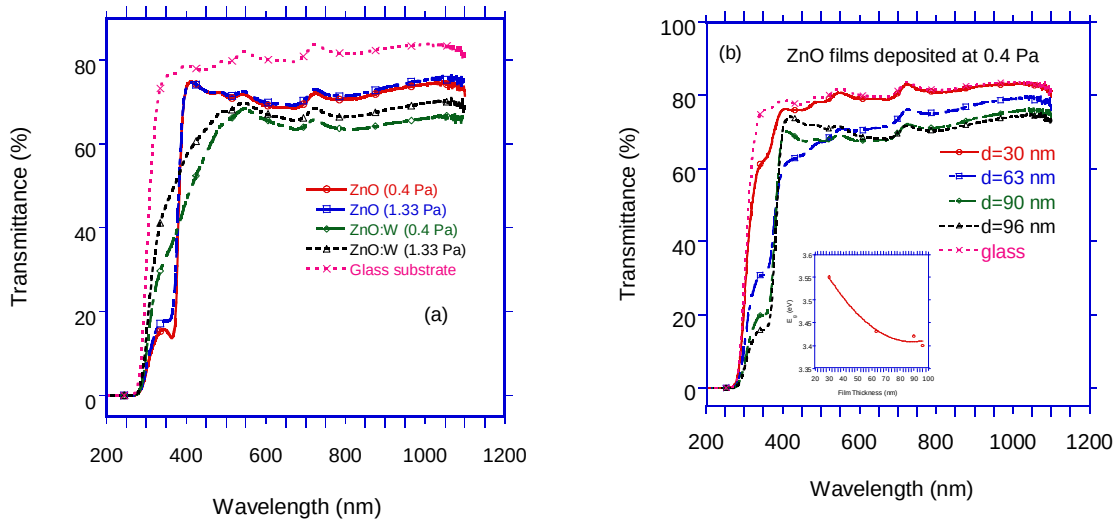

Fig. 5 (a) Spectral transmittance of pure and W-doped ZnO films on glass substrate deposited at 0.4 Pa and 1.33 Pa. (a) Effect of doping at two sputtering pressures, and (b) effect of film thickness on the transmittance and optical band gap of the pure ZnO film.

The sensing performances of the pure and W-doped ZnO films annealed at 400°C towards 1-10 ppm NO_2 gas at the operating temperature of 150-300°C were examined. Only three of the four samples have shown a response to NO_2 at 5 and 10 ppm as shown in Fig. 6. From the figure, a noticeable response can be observed from the pure ZnO films. However, the response of the ZnO film deposited at 0.4 Pa has been improved significantly after doped with W and this is much more apparent at lower operating temperature (nearly 8 times at 150°C). There was no response observed from the W-doped ZnO film deposited at 1.33 Pa due to very high resistance of the film (see Table 3). The reason for such high film resistance is not clear but from XPS the surface of this film was dominated by adsorbed oxygen species compared to the O-Zn bonding and

favoured the adsorption of OH species [46] and the surface contaminant may be the main cause for such high resistance. In addition, the film appeared to have less porousity and fewer grains (see Fig. 2d), and such morphologies are undesirable for enhanced gas sensing properties.

As shown in Fig. 7, the response of the films is higher at lower operating temperature (150°C) and decreases with increasing temperature. The W-doped ZnO film deposited at 0.4 Pa exhibited high response amplitude (sensitivity) of 350 towards 10 ppm NO_2 gas at operating temperature of 150°C. The response and recovery times of the sensors at 5 ppm and 10 ppm NO_2 gas in the operating temperature of 150-250°C are shown in Table 4. As expected the response and recovery times generally decrease with increasing temperature and increasing gas concentration. From the overall results, the sensing performance of ZnO film without the presence of OH contaminates has shown markedly high senstivity at lower operting temperature after doped with W and this is most likely due to enhanced free-carrier defects of the W-doped ZnO film obtained by sputtering at lower power.

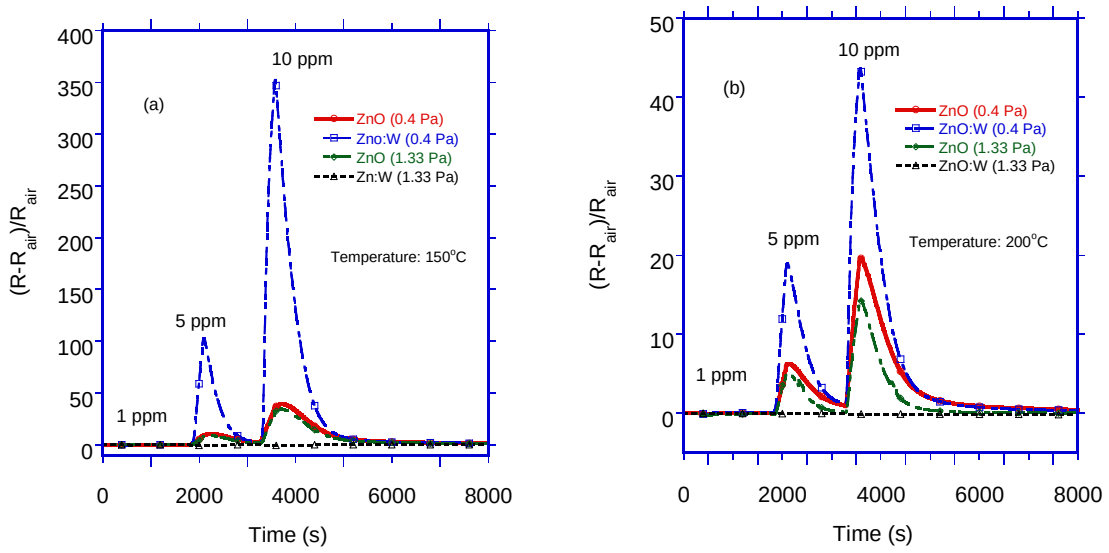

Fig. 6 Dynamic response of pure and W-doped ZnO films towards various concentrations of NO_2 gas (1, 5, 10 ppm) measured at operating temperature of (a) 150°C and (b) 200°C.

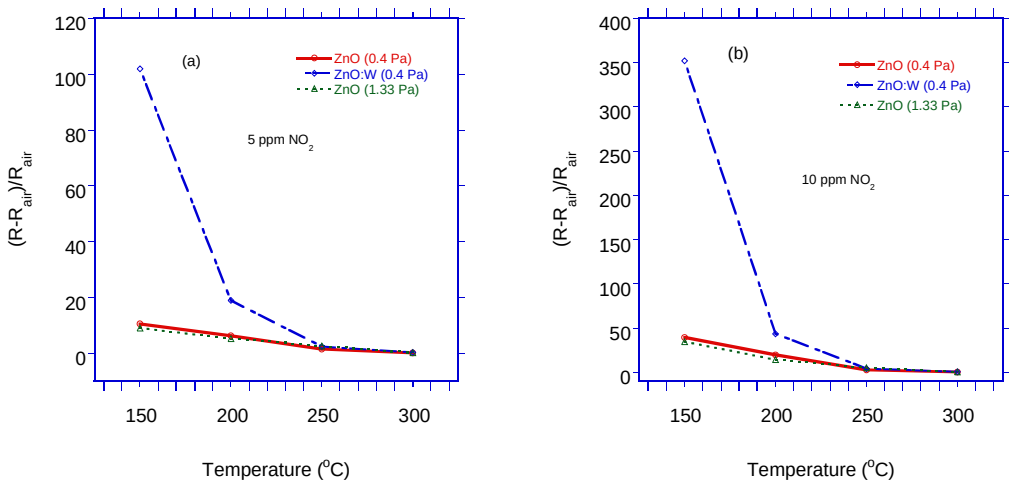

Fig. 7 Response amplitude (sensitivity) of pure and W-doped ZnO films towards 5 and 10 ppm NO_2 at operating temperature of 150-300°C.

Table 4: Response and recovery times of the pure and W-doped ZnO films to 5 ppm and 10 ppm NO_2 gas at different operating temperature (150-250°C).

Temperature	ZnO (0.4 Pa)	ZnO (1.33 Pa)	ZnO:W (0.4 Pa)	ZnO (0.4 Pa)	ZnO (1.33 Pa)	ZnO:W (0.4 Pa)
	Response time at 5 ppm			Recovery time at 5 ppm		
150 (°C)	300 s	270 s	195 s	1000 s	690 s	650 s
200 (°C)	240 s	280 s	200 s	920 s	770 s	750 s
250 (°C)	230 s	260 s	275 s	590 s	820 s	630 s
	Response time at 10 ppm					
150 (°C)	265 s	255 s	220 s	1200 s	855 s	845 s
200 (°C)	280 s	230 s	210 s	1200 s	845 s	955 s
250 (°C)	215 s	250 s	250 s	650 s	830 s	700 s

Conclusions

Pure and W-doped ZnO thin films were deposited using lower sputtering power (30 W RF and 10 W DC) at pressure of 0.4 Pa and 1.33 Pa. The films were deposited at room temperature and subsequently annealing at 400°C for 1 hour in air. Doping and annealing assisted the formation of grains whereas higher sputtering pressure (1.33 Pa) produced spike-like grains. From AFM the average grain size and surface roughness of the annealed samples were 65 nm and 2.2 nm, respectively. Raman spectra indicated more free-carrier defects were induced by W-dopant due to breakdown of the translational crystalline symmetry of the pure ZnO film and this was supported from optical measurements. When the doped films were compared, the film deposited at 1.33 Pa

was found to have lower oxidation state of W and surface dominated adsorbed oxygen species compared to the O-Zn bonding found in the film deposited at 0.4 Pa. This adsorbed oxygen species favoured active surface sites for OH adsorption and caused unfavourable film properties for NO_2 gas sensing. The W-doped ZnO film deposited at 0.4 Pa has shown enhanced gas sensing performance (up to 8 times) towards 5-10 ppm NO_2 at lower temperature (150^oC). From the overall results it is concluded that the high sensing performance of the W-doped ZnO sensor to NO_2 gas at lower operating temperature (150^oC) was most like achieved due to the enhanced free-carrier defects of the film obtained using lower sputtering power at pressure of 0.4 Pa.

Acknowledgments

This work has financially supported by Japanese Society for the Promotion of Science (JSPS). AFM characterisation has been made at the Laboratory of Nanosciences and Materials at Hokkaido University (Japan). This research was done at IFE Central Analytical Research Facility at QUT.

References

[1] L.J. LeGore, R.J. Lad, S.C. Moulzolf, J.F. Vetelino, B.G. Frederick, E.A. Kenik, Defects and morphology of tungsten trioxide thin films, Thin Solid Films, 406 (2002) 79-86.
[2] N. Evcimen Duygulu, A.O. Kodolbas, A. Ekerim, Effects of argon pressure and r.f. power on magnetron sputtered aluminum doped ZnO thin films, Journal of Crystal Growth, 394 (2014) 116-125.
[3] A. Axelevitch, B. Gorenstein, H. Darawshe, G. Golan, Investigation of thin solid ZnO films prepared by sputtering, Thin Solid Films, 518 (2010) 4520-4524.
[4] X.B. Wang, C. Song, K.W. Geng, F. Zeng, F. Pan, Photoluminescence and Raman scattering of Cu-doped ZnO films prepared by magnetron sputtering, Applied Surface Science, 253 (2007) 6905-6909.
[5] H.S. Al-Salman, M.J. Abdullah, Fabrication and characterization of ZnO thin film for hydrogen gas sensing prepared by RF-magnetron sputtering, Measurement, 46 (2013) 1698-1703.
[6] E. Heredia, C. Bojorge, J. Casanova, H. Cánepa, A. Craievich, G. Kellermann, Nanostructured ZnO thin films prepared by sol–gel spin-coating, Applied Surface Science, 317 (2014) 19-25.
[7] T.-L. Phan, S.C. Yu, R. Vincent, N.H. Dan, W.S. Shi, Photoluminescence properties of various CVD-grown ZnO nanostructures, Journal of Luminescence, 130 (2010) 1142-1146.
[8] A.R. Bari, L.A. Patil, I.G. Pathan, D.N. Surawanshi, D.S. Rane, Characterizations of Ultrasonically Prepared Nanostructured ZnO powder and NH3 Sensing Performance of its Thick Film Sensor, Procedia Materials Science, 6 (2014) 1798-1804.
[9] Q.A. Drmosh, S.G. Rao, Z.H. Yamani, M.A. Gondal, Crystalline nanostructured Cu doped ZnO thin films grown at room temperature by pulsed laser deposition technique and their characterization, Applied Surface Science, 270 (2013) 104-108.

[10] M. Shirazi, M.T. Hosseinnejad, A. Zendehnam, M. Ghoranneviss, G. Reza Etaati, Synthesis and characterization of nanostructured ZnO multilayer grown by DC magnetron sputtering, Journal of Alloys and Compounds, 602 (2014) 108-116.
[11] F.Z. Bedia, A. Bedia, N. Maloufi, M. Aillerie, F. Genty, B. Benyoucef, Effect of tin doping on optical properties of nanostructured ZnO thin films grown by spray pyrolysis technique, Journal of Alloys and Compounds, 616 (2014) 312-318.
[12] I. Mihailova, V. Gerbreders, E. Tamanis, E. Sledevskis, R. Viter, P. Sarajevs, Synthesis of ZnO nanoneedles by thermal oxidation of Zn thin films, Journal of Non-Crystalline Solids, 377 (2013) 212-216.
[13] G. Kenanakis, N. Katsarakis, Ultrasonic spray pyrolysis growth of ZnO and ZnO:Al nanostructured films: Application to photocatalysis, Materials Research Bulletin, 60 (2014) 752-759.
[14] A. Ismail, M.J. Abdullah, The structural and optical properties of ZnO thin films prepared at different RF sputtering power, Journal of King Saud University - Science, 25 (2013) 209-215.
[15] S. Flickyngerova, K. Shtereva, V. Stenova, D. Hasko, I. Novotny, V.Tvarozek, P. Sutta, E. Vavrinsky, Structural and optical properties of sputtered ZnO thin films, Applied Surface Science, 254 (2008) 3643-3647.
[16] V. Bhatt, P. Pal, S. Chandra, Feasibility study of RF sputtered ZnO film for surface micromachining, Surface and Coatings Technology, 198 (2005) 304-308.
[17] W. Water, S.-Y. Chu, Physical and structural properties of ZnO sputtered films, Materials Letters, 55 (2002) 67-72.
[18] T. Tesfamichael, C. Piloto, M. Arita, J. Bell, Fabrication of Fe-doped WO3 films for NO2 sensing at lower operating temperature, Sensors and Actuators B: Chemical, 221 (2015) 393-400.
[19] M. Ahsan, T. Tesfamichael, A. Ponzoni, G. Faglia, Sensing properties of e-beam evaporated nanostructured pure and iron-doped tungsten oxide thin films, Sens. Lett., 9 (2011) 759-762.
[20] T. Tesfamichael, N. Motta, T. Bostrom, J.M. Bell, Development of porous metal oxide thin films by co-evaporation, Appl Surf Sci, 253 (2007) 4853-4859.
[21] Z.B. Ayadi, L. El Mir, K. Djessas, S. Alaya, The properties of aluminum-doped zinc oxide thin films prepared by rf-magnetron sputtering from nanopowder targets, Materials Science and Engineering: C, 28 (2008) 613-617.
[22] S.J. Kang, Y.H. Joung, Influence of substrate temperature on the optical and piezoelectric properties of ZnO thin films deposited by rf magnetron sputtering, Applied Surface Science, 253 (2007) 7330-7335.
[23] J.-j. Zhang, E.-j. Guo, L.-p. Wang, H.-y. Yue, G.-j. Cao, L. Song, Effect of annealing treatment on morphologies and gas sensing properties of ZnO nanorods, Transactions of Nonferrous Metals Society of China, 24 (2014) 736-742.
[24] C.-H. Choi, S.-H. Kim, Effects of post-annealing temperature on structural, optical, and electrical properties of ZnO and Zn1−xMgxO films by reactive RF magnetron sputtering, Journal of Crystal Growth, 283 (2005) 170-179.
[25] G.P. Daniel, V.B. Justinvictor, P.B. Nair, K. Joy, P. Koshy, P.V. Thomas, Effect of annealing temperature on the structural and optical properties of ZnO thin films prepared by RF magnetron sputtering, Physica B: Condensed Matter, 405 (2010) 1782-1786.
[26] H.H.P.T. Bekman, K.W. Benoist, J.L. Joppe, Post-deposition annealing of RF-sputtered zinc-oxide films, Applied Surface Science, 70–71, Part 1 (1993) 347-350.

[27] O. Lupan, G. Chai, L. Chow, Fabrication of ZnO nanorod-based hydrogen gas nanosensor, Microelectronics Journal, 38 (2007) 1211-1216.
[28] X.Q. Zhao, C.R. Kim, J.Y. Lee, C.M. Shin, J.H. Heo, J.Y. Leem, H. Ryu, J.H. Chang, H.C. Lee, C.S. Son, B.C. Shin, W.J. Lee, W.G. Jung, S.T. Tan, J.L. Zhao, X.W. Sun, Effects of thermal annealing temperature and duration on hydrothermally grown ZnO nanorod arrays, Applied Surface Science, 255 (2009) 5861-5865.
[29] V.A. Minh, L.A. Tuan, T.Q. Huy, V.N. Hung, N.V. Quy, Enhanced NH3 gas sensing properties of a QCM sensor by increasing the length of vertically orientated ZnO nanorods, Applied Surface Science, 265 (2013) 458-464.
[30] S. Bai, T. Guo, Y. Zhao, J. Sun, D. Li, A. Chen, C.C. Liu, Sensing performance and mechanism of Fe-doped ZnO microflowers, Sensors and Actuators B: Chemical, 195 (2014) 657-666.
[31] M. Xu, Q. Li, Y. Ma, H. Fan, Ni-doped ZnO nanorods gas sensor: Enhanced gas-sensing properties, AC and DC electrical behaviors, Sensors and Actuators B: Chemical, 199 (2014) 403-409.
[32] X. Jia, H. Fan, M. Afzaal, X. Wu, P. O'Brien, Solid state synthesis of tin-doped ZnO at room temperature: Characterization and its enhanced gas sensing and photocatalytic properties, Journal of Hazardous Materials, 193 (2011) 194-199.
[33] J.-Q. He, J. Yin, D. Liu, L.-X. Zhang, F.-S. Cai, L.-J. Bie, Enhanced acetone gas-sensing performance of La2O3-doped flowerlike ZnO structure composed of nanorods, Sensors and Actuators B: Chemical, 182 (2013) 170-175.
[34] C. Zhang, X.-l. Chen, X.-h. Geng, C.-s. Tian, Q. Huang, Y. Zhao, X.-d. Zhang, Temperature-dependent growth and properties of W-doped ZnO thin films deposited by reactive magnetron sputtering, Applied Surface Science, 274 (2013) 371-377.
[35] J. Chu, X.Y. Peng, K. Dasari, R. Palai, P. Feng, The shift of optical band gap in W-doped ZnO with oxygen pressure and doping level, Materials Research Bulletin, 54 (2014) 73-77.
[36] H. Zhang, H. Liu, C. Lei, C. Yuan, A. Zhou, Vacuum, 85 (2010) 184.
[37] B.D. Ngom, O. Sakho, N. Manyala, J.B. Kana, N. Mlungisi, L. Guerbous, A.Y. Fasasi, M. Maaza, A.C. Beye, Appl. Surf. Sci., 255 (2009) 7314.
[38] M. Stankova, X. Vilanova, J. Calderer, E. Llobet, J. Brezmes, I. Gràcia, C. Cané, X. Correig, Sensitivity and selectivity improvement of rf sputtered WO3 microhotplate gas sensors, Sens. Actuators B Chem, 113 (2006) 241-248.
[39] O. Berger, T. Hoffmann, W.-J. Fischer, V. Melev, Tungsten-oxide thin films as novel materials with high sensitivity and selectivity to NO2, O3, and H2S. Part II: Application as gas sensors, J. Mater. Sci: Mater. Elect. , 15 (2004) 483-493.
[40] K. Saravanakumar, C. Gopinathan, K. Mahalakshmi, V. Ganesan, V. Sathe, C. Sanjeeviraja, XPS and Raman Studies on (002) Oriented Nanocrystalline ZnO Films Showing Temperature Dependent Optical Red Shift, Adv. Studies Theor. Phys., 5 (2011) 155-170.
[41] F.J. Manjón, B. Marí, J. Serrano, A.H. Romero, Silent Raman modes in zinc oxide and related nitrides J. Appl. Phys., 97 (2005) 053516.
[42] H.C. Barshilia, N. Selvakumar, N. Pillai, L.M. Devi, K.S. Rajam, Wettability of ZnO: A comparison of reactively sputtered; thermally oxidized and vacuum annealed coatings, Applied Surface Science, 257 (2011) 4410-4417.
[43] G. Gottardi, R. Bartali, V. Micheli, N. Laidani, D. Avi, Role of hydrogen addition in the plasma phase in determining the structural and chemical properties of RF sputtered ZnO films, Materials Chemistry and Physics, 127 (2011) 364-370.

[44] L.-J. Meng, C.P. Moreira de Sá, M.P. dos Santos, Study of the structural properties of ZnO thin films by x-ray photoelectron spectroscopy, Applied Surface Science, 78 (1994) 57-61.
[45] M. Chen, X. Wang, Y.H. Yu, Z.L. Pei, X.D. Bai, C. Sun, R.F. Huang, L.S. Wen, X-ray photoelectron spectroscopy and auger electron spectroscopy studies of Al-doped ZnO films, Applied Surface Science, 158 (2000) 134-140.
[46] L.L. Yang, Q.X. Zhao, M. Willander, X.J. Liu, M. Fahlman, J.H. Yang, Origin of the surface recombination centers in ZnO nanorods arrays by X-ray photoelectron spectroscopy, Applied Surface Science, 256 (2010) 3592-3597.
[47] M.M. Can, T. Fırat, S. Ismat Shah, Magnetoelectrical properties of W doped ZnO thin films, Journal of Magnetism and Magnetic Materials, 324 (2012) 4054-4060.
[48] F.K. Shan, Y.S. Yu, Band gap energy of pure and Al-doped ZnO thin films, Journal of the European Ceramic Society, 24 (2004) 1869-1872.
[49] J. Tauc, Amorphous and Liquid Semiconductors, Plenum Press, London, 1974.
[50] A.Z. Moshfegh, R. Azimirad, O. Akhavan, Optical properties and surface morphology of evaporated WO_3-Fe_2O_3 thin films, Thin Solid Films, 484 (2005) 124-131.
[51] W.M. Kim, J.S. Kim, J.-h. Jeong, J.-K. Park, Y.-J. Baik, T.-Y. Seong, Analysis of optical band-gap shift in impurity doped ZnO thin films by using nonparabolic conduction band parameters, Thin Solid Films, 531 (2013) 430-435.